ELSEVIER

Contents lists available at ScienceDirect

Journal of Colloid And Interface Science

journal homepage: www.elsevier.com/locate/jcis



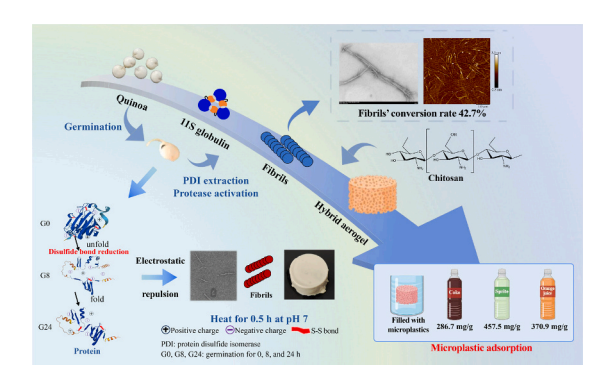


Germination-induced nanoarchitectonic assembly of quinoa protein at neutral pH and its aerogels for microplastic removal

Xiao Feng ^a, Lixiao Fu ^a, Jianfeng Wei ^a, Chaosheng Wu ^a, Hui Zhang ^b, Lin Chen ^c, Xi Yu ^d, Yuan Li ^{b,*}, Xiaozhi Tang ^{a,**}

- ^a College of Food Science and Engineering/Collaborative Innovation Center for Modern Grain Circulation and Safety/Key Laboratory of Grains and Oils Quality Control and Processing, Nanjing University of Finance and Economics, Nanjing 210023, China
- b Research Center of Food Colloids and Delivery of Functionality, College of Food Science and Nutritional Engineering, China Agricultural University, Beijing 100094, China
- ^c School of Chemistry, Chemical Engineering and Biotechnology, Nanyang Technological University, Singapore 637459, Singapore
- d Faculty of Medicine, Macau University of Science and Technology, Avenida Wai Long Taipa, Macau 999078, China

GRAPHICAL ABSTRACT



ARTICLE INFO

Keywords:
Quinoa protein
Germination
Amyloid-like fibrils
Protein disulfide isomerase
Aerogels
Microplastic removal

$A\ B\ S\ T\ R\ A\ C\ T$

Microplastics (MPs) have emerged as a growing concern due to their potential threats to human health and aquatic systems. Aerogels have shown promise for MP removal. However, low-cost, plant-derived aerogels remain underexplored. Plant proteins typically exhibit weak gelling capacity, limiting their utility in forming porous structures. Although acidic conditions (pH 2) have been used to induce protein fibrillation and enhance gelation, such methods are energy-intensive and environmentally unfavorable. In this study, we developed a sustainable and efficient strategy to induce quinoa protein fibrillation under neutral pH conditions via seed germination. Quinoa protein isolate (QPI) extracted from quinoa seeds germinated for 8 h formed fibrils (200–800 nm) upon thermal treatment at 95 °C for 30 min at pH 7. Germination improved the electronegativity of QPI to -30.6 mV, and reduced disulfide bonding via protein disulfide isomerase, promoting electrostatic

E-mail address: yuanli@cau.edu.cn (Y. Li).

https://doi.org/10.1016/j.jcis.2025.139058

^{*} Corresponding author at: Research Center of Food Colloids and Delivery of Functionality, College of Food Science and Nutritional Engineering, China Agricultural University, Beijing 100094, China.

^{**} Corresponding author at: College of Food Science and Engineering, Nanjing University of Finance and Economics, No. 3 Wenyuan Road, Nanjing, Jiangsu Province 210023, China.

repulsion and molecular unfolding to facilitate fibril formation. Inspired by germination, synergistic enzymatic strategy was discovered to induce 11S globulin fibrillation with enhanced fibrils' conversion rate of 42.7 % under neutral condition. The resulting fibril-based aerogels demonstrated efficient microplastic removal from both water and beverage systems, and their adsorption capacity reached 286.7 mg/g in coke, 457.5 mg/g in Sprite, and 370.9 mg/g in orange juice, highlighting their potential as low-cost, plant-based materials for microplastic removal.

1. Introduction

Microplastics (MPs) have been recognized as pervasive environmental contaminants, with their prevalence in atmospheric, soil, and aquatic ecosystems. Microplastics induce oxidative stress, disrupt metabolism, interfere with gut microflora and gastrointestinal functions, disrupt cardiopulmonary, hepatic and immune systems, and affect reproductive health [1,2]. The global burden of MPs is projected to rise significantly, from 41 kt in 2000 to an estimated 1397 kt by 2060. Aerogels have been reported to remove microplastics from water, such as polydopamine/chitosan aerogels, reduced graphene oxide aerogels, and egg white aerogels [3]. Comparing with polydopamine and reduced graphene oxide with high price, plant proteins are cost-effective, and they are also biodegradable [1]. Oat-amyloid aerogels were fabricated for water treatment [4]. However, their effect on microplastic removal was not revealed. Meanwhile, amyloid-like fibrils formed under strong acidic conditions are susceptible to pH changes, and strong acids are not favorable to environment and industrial application. Therefore, alternative methods should be sought to promote the fibrillation of plant proteins to structure plant-based aerogels.

Among various plants, naturally stress-resistant crops have been receiving more and more attention due to climate changes and soil salinity, which is beneficial for sustainable agriculture [5]. Quina belongs to naturally stress-resistant crops. Like most of the plant proteins, quinoa protein has a weak gelling property, limiting its application as aerogels. It was reported that plant proteins can be hydrolyzed and form amyloid-like fibrils when heated at pH 2 [6]. The fibrillation of proteins provides more regions to cross-link proteins to form a networking structure with improved gelling property.

Quinoa germinates rapidly under mild conditions [7], which exploits favorable conditions as a means of survival for seeds from high stress habitats [8]. Compared with physical, chemical and enzymatic modifications, germination is a green, environmentally friendly, low-cost approach to hydrolyze and synthesize new proteins [9]. Germination

may partially hydrolyze quinoa protein, change its conformation and properties, and promote the rearrangement and assembly. This may shed new light on the fibrillation of quinoa protein under mild conditions. This hypothesis is shown in Fig. 1.

In this study, the fibrillation of quinoa proteins under neutral pH induced by germination was discovered and reported for the first time. Meanwhile, the effects of germination on the physicochemical properties of QPIs were comprehensively studied to explain its fibrillation. Moreover, the effects of germination on the gel microstructure, rheological properties were also explored. Furthermore, inspired by germination, synergistic enzymatic approaches were firstly applied to induce the fibrillation of quinoa 11S globulin to enhance the fibrils' conversion rate and generate functional aerogels to remove microplastics in water and beverages. This study provides theoretical basis to structure quinoa protein aerogels with promising microplastic removal efficiency via green strategies and sheds light on the microplastic removal in vitro.

2. Materials and methods

2.1. Materials

Quinoa was purchased from Beijing Jinhe Luyuan Trading Co., Ltd. (Beijing, China). Bromelain, enzyme activity of 600 units/mg protein, was obtained from Shanghai Yuanye Bio-Technology Co., Ltd. (Shanghai, China). All chemicals are of analytical grade.

2.2. Quinoa seed germination

The germination of quinoa seeds was based on Liu et al. [10] with some modifications. Quinoa seeds (200 g) were sterilized in sodium hypochlorite solution (10 g/L) for 10 mins and then thoroughly rinsed with deionized water. The sterilized seeds were soaked in $\rm H_2O_2$ solution (10 g/L) and germinated in the dark at 25 °C. The samples were collected every 8 h, named G0, G8, G16, and G24, and were

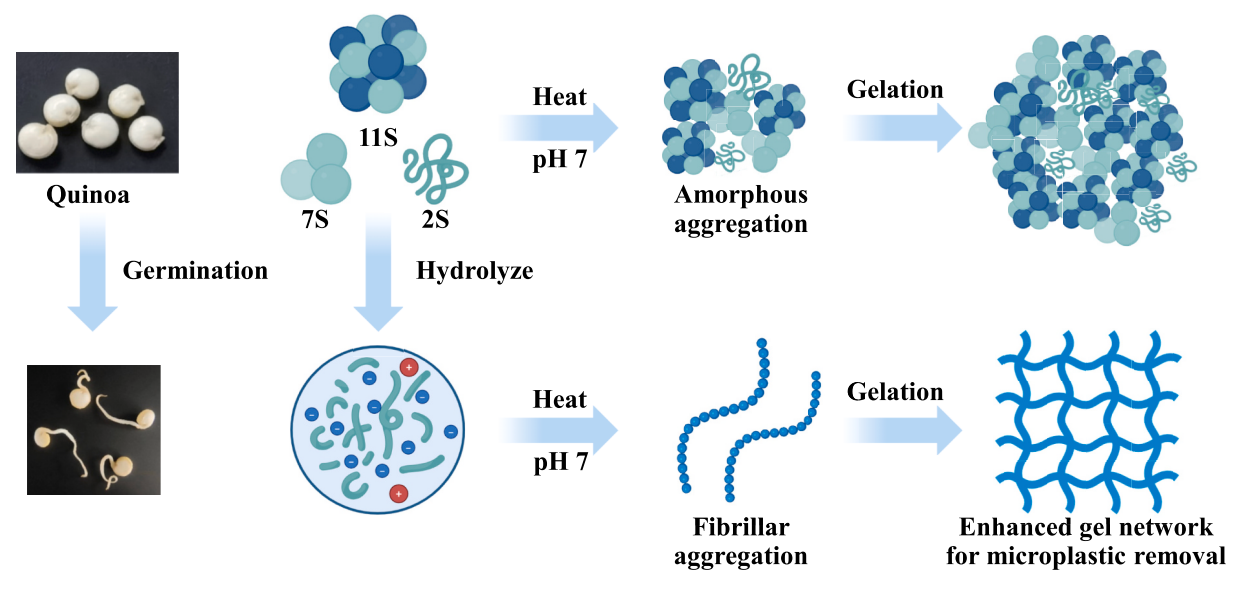


Fig. 1. Hypothesis of this research.

photographed. After germination, the seeds were first dried at $40\pm5~^\circ\mathrm{C}$ for 12~h and then ground into powders followed by sieving. The quinoa powders were mixed with n-hexane at a ratio of 1:3 (w:v) and defatted for 2 h, which was repeated three times. The defatted quinoa powder was dried overnight in a fume hood to completely evaporate the residual n-hexane.

2.3. Quinoa protein isolate extraction

QPI was extracted from defatted quinoa flour according to the method of Yang et al. [11] with slight modifications. Defatted quinoa flour was suspended in Milli-Q water at a volume ten times that of the flour, and the pH was adjusted to 8.5 using 1 mol/L NaOH. The suspension was stirred at room temperature for 2 h. The mixture was then centrifuged at $10,000 \times g$ for 15 min at 4 °C to obtain the supernatant, and the pH was adjusted to 4.5 to precipitate proteins. The mixture was then centrifuged at $10,000 \times g$ for 15 min at 4 °C to recover the protein pellet, which was dissolved in Milli-Q water and neutralized to pH 7 using 1 mol/L NaOH. The QPI solution was frozen at -80 °C for 12 h, followed by freeze-drying. The freeze-dried powders were ground into fine particles and stored at 4 °C.

2.4. Preparation of QPI aggregates

QPI extracted from quinoa germinated for different time was dissolved in Milli-Q water to prepare a suspension (20 mg/mL). The protein isolates from ungerminated quinoa were adjusted to pH 2 and 7, while those from quinoa germinated for 8, 16, and 24 h were adjusted to pH 7. All samples were stirred at room temperature for 2 h and then heated in a sealed glass bottle in a 95 $^{\circ}\text{C}$ water bath for 30 min, followed by rapid cooling in an ice-water bath. QPI aggregates were then stored at 4 $^{\circ}\text{C}$ for further experiments.

2.5. Thioflavin T (ThT) fluorescence analysis

ThT fluorescence intensity was measured according to Nilsson [12]. ThT of 8 mg was dissolved in 10 mL of phosphate buffer (pH 7, 150 mmol/L NaCl) to prepare ThT stock solution. A 0.22 μm filter membrane was applied to remove the undissolved particles. The stock solution was stored in the dark at 4 °C and diluted 50-fold prior to each measurement. Samples of 50 μL were mixed with 5 mL of ThT working solution for at least 1 min. A fluorescence spectrophotometer (Hitachi Ltd., Tokyo, Japan) was used for ThT fluorescence measurement. The relative ThT fluorescence intensity of the sample was determined by subtracting the fluorescence intensity of the ThT working solution.

2.6. Negative stain transmission electron microscopy

The morphology of the QPI aggregates was measured by TEM. Prior to sample fixation, a 230-mesh carbon-coated copper grid was glow-discharged for 45 s to enhance sample resolution. QPI aggregation solution (10 mg/mL) of 10 μL was evenly applied to the copper grid and incubated for 1 min, followed by an additional incubation with 2 % uranyl acetate for 30 s. After each step, excess water was blotted with filter paper along the periphery. Transmission electron microscopy images were obtained using a 120 kV TEM (HITACHI H-7650, Tokyo, Japan) [6].

2.7. Atomic force microscopy (AFM)

The morphology of the QPI aggregates was measured by AFM following a previously described method with some modifications [13]. The protein concentration was diluted to 1 g/L using Milli-Q water at the same pH as the sample. Diluted sample of 10 μL was deposited onto a freshly cleaved mica surface and air-dried after being washed three times with Milli-Q water. Images were obtained using AFM (HR-AFM,

AFM workshop Hangzhou, China) and a tap 190 cantilever in tapping mode. The scanning rate was $1\ Hz$.

2.8. Physicochemical properties of QPIs

2.8.1. Degree of hydrolysis (DH), protein composition, and solubility of OPIs

The DH of QPIs was determined with slight modifications based on the method described by Nielsen et al. [14]. Briefly, 0.1 g of freeze-dried powder was dissolved in 100 mL of Milli-Q water, and 400 μ L of the solution was mixed with 3 mL of OPA reagent. The mixture was stirred for 5 s and allowed to stand for 2 min at room temperature, and then the absorbance was measured at 340 nm using a spectrophotometer (U-3900, Hitachi, Japan). L-serine solution (0.9516 meqv/L) was used as a standard, and Milli-Q water was used as a blank sample. Each sample was measured in triplicate. The calculation was performed as follows:

$$DH (\%) = \frac{h}{h_{tot}} \times 100 \tag{1}$$

$$h = \frac{\text{Serine NH}_2 - \beta}{\alpha} \tag{2}$$

 h_{tot} is 8 mequv/g, and β and α are 0.4 mequv/g and 1 mequv/g, respectively.

SDS-PAGE was used to analyze the changes in the protein composition of quinoa at different germination time. The solubility of QPIs extracted from different quinoa seeds was determined according to Di et al. [15].

2.8.2. Surface hydrophobicity, zeta potential, total/free sulfhydryl groups and disulfide bonds of QPIs

The surface hydrophobicity (H₀) was determined with slight modifications according to Di et al. [15]. QPI samples were diluted to concentrations of 12.5, 25, 50, 100, and 200 μ g/mL in 10 mmol/L Tris-HCl buffer (pH 7). Subsequently, 3 mL of each sample was mixed with 50 μL of 8.0 mmol/L ANS solution and incubated in the dark at room temperature for 20 min. The fluorescence intensities were recorded using a Shimadzu RF-9000 fluorescence spectrophotometer (Kyoto, Japan). The surface hydrophobicity (H₀) of the protein samples was expressed as the initial slope of the relative fluorescence intensity plotted against the protein concentration for various dilutions. The determination of zeta potential was performed using a nanoparticle size analyzer (Nano-ZS90, Malvern Instruments, Malvern, UK). OPI was dispersed in Milli-O water (0.5 mg/mL), and the pH was adjusted to 7, followed by measuring the surface charge. Each sample was measured three times. The measurement of the total and sulfhydryl (-SH) groups and the disulfide bond content in QPI was based on Anderson et al. [16].

2.9. Gastrointestinal digestion of QPI aggregates

According to Lassé et al. [17], the digestion of QPI aggregates (G0 pH 2, G0 pH 7, G8 pH 7) in simulated gastric fluid (SGF) and simulated intestinal fluid (SIF) was carried out. QPI aggregates (20 mg/mL, 3 mL) were resuspended in SGF (7 mL) and incubated for 2 h on a shaker at 150 rpm and 37 °C. Thereafter, the pH was adjusted to 7. Subsequently, an equal volume of SIF was added and reacted for 2 h. Then, the intestinal phase was treated at 90 °C for 10 min to inactivate the enzyme. The ThT fluorescence intensity and the morphology of aggregates after digestion were measured according to the method mentioned above.

2.10. Cytotoxicity evaluation of QPI aggregates and their digest

The cytotoxicity of representative QPI aggregates, G0 (pH 2), G0 (pH 7) and G8 (pH 7), was determined by a cell counting kit-8 assay (CCK-8) [13,17,18]. MODE-K cells were cultured in Dulbecco's modified Eagle's medium (DMEM) containing 100 mg/mL fetal bovine serum (FBS) and

10 mg/mL penicillin/streptomycin at 37 °C under 5 % (ν /v) CO₂. To examine the cell cytotoxicity of different samples before and after gastrointestinal digestion, different samples (18 mg) were digested according to the methods mentioned above. The digestive juices were diluted to final protein concentrations of 1000, 800, 600, 400, 200, 100, 50, and 25 μ g/mL. MODE-K cells seeded in 96-well plates were incubated with various concentrations (0, 25, 50, 100, 200, 400, 600, 800, 1000 μ g/mL) of G0 (pH 2), G0 (pH 7), G8 (pH 7) samples, and the digesting diluent of G0 (pH 2) and G8 (pH 7) samples for 24 h. The CCK-8 assay was carried out to determine the cell viabilities. The absorbance at 450 nm was measured using a multimode plate reader (BioTek Instruments, Inc., USA).

2.11. Extraction of protein disulfide isomerase from germinated quinoa seeds

Protein disulfide isomerase was extracted from 8 h germinated quinoa seeds as it showed the strongest disulfide bond reduction activity as shown in Fig. 3F. Quinoa seeds germinated for 8 h were dried and then ground using liquid nitrogen. Six grams of the grounded powder were placed in a 50 mL centrifuge tube, and 18 mL of buffer A (20 mmol/L 4-(2-hydroxyethyl)-1-piperazinyl-ethanesulfonic acid (pH 7.5), 150 mmol/L NaCl, 2 mmol/L CaCl₂) was added. The mixture was quickly stirred at 4 °C for 10 min, and was then centrifuged at 10,000 g for 20 min at 4 °C to collect the supernatant. Thereafter, 6.7 g of ammonium sulfate was added to the supernatant, and the solution was stirred until fully dissolved, then placed at 4 °C to precipitate overnight. After centrifugation at 10,000 g for 40 min at 4 °C, the precipitate was collected and completely dissolved in 1.6 mL of buffer A. The resulting protein solution was placed in a dialysis bag and subjected to two rounds of dialysis. Finally, the solution was centrifuged at 10,000 g for 10 min at 4 °C, and the supernatant obtained was PDI dispersion [19], which was then stored at 4 $^{\circ}\text{C}$ and used within one week.

2.12. Preparation of quinoa 11S globulin fibrils by synergistic enzymatic method

Prepare 11S globulin dispersion of 25 mg/mL, which was hydrated in an ice-water bath for 2 h and then stored overnight at 4 °C. Thereafter, the pH was readjusted to 7.0, and the dispersion was heated in a water bath at 55 °C for 10 min. Bromelain was added at a substrate-to-enzyme ratio of 0.025 %, and hydrolysis was allowed to proceed for 3 min before the addition of PMSF, which is the protease inhibitor [20]. The hydrolyzed sample was then placed in a water bath at 40 °C and treated with 0.5 mL of disulfide isomerase for 4 h, followed by the addition of the disulfide isomerase inhibitor CCF642 to halt the reduction reaction [21]. Finally, the protein hydrolysate solution was heated in a water bath at 95 °C for 1 h to induce the formation of 11S globulin nanofibrils and then rapidly cooled in an ice-water bath before being stored at 4 °C for future use.

2.13. Conversion rate of fibrils

Trypsin (enzymatic activity≥250 units/mg protein) was added to the 11S globulin aggregate solutions to disrupt the amorphous aggregates at 37 °C [22], which was then inhibited by PMSF after 4 h of reaction. The resulting samples (2 mg/mL) were added to centrifugal filters (100 kDa, MWCO, Merck Millipore, USA), and centrifuged at 3000 g for 15 min. The filtrate was referred to as "fraction 1". The retentate was washed with Milli-Q water twice, and the resulting filtrates were referred to as "fraction 2" and "fraction 3", respectively. The volume of the filtrate was measured, and the protein concentration of the fractions was determined. The conversion rate was calculated by the following Eq. [23].

$$C = \frac{F - (F_1 + F_2 + F_3)}{F} \times 100\% \tag{3}$$

F (g) is the protein content of diluted samples. F1, F2, F3 (g) is the protein content of fraction 1, fraction 2 and fraction 3, respectively.

2.14. Aerogels prepared from quinoa 11S globulin fibrils

Firstly, quinoa 11S globulin hydrogel, chitosan hydrogel, and their composite hydrogel were prepared accordingly. The quinoa 11S globulin (40 mg/mL) was suspended in NaCl solution (20 mmol/L), which was subjected to bromelain hydrolysis and PDI reduction, followed by ultrasonic treatment. It was heated in a water bath at 95 °C for 1 h to prepare the 11S globulin fibril hydrogels [24]. Chitosan powder was dissolved in 30 mL/L acetic acid aqueous solution until the solution became clear, resulting in a final chitosan concentration of 40 mg/mL. The chitosan solution was then mixed with glutaraldehyde solution (20 mL/L), stirred thoroughly, and left overnight at 4 °C in a refrigerator to generate chitosan hydrogels [25]. Thereafter, quinoa 11S globulin fibrils and chitosan composite hydrogels were prepared. The quinoa 11S globulin fibril solution (30 mg/mL) and chitosan (CS) solution (40 mg/ mL) were mixed in different ratios (1:1, 2:1, 3:1) (300 rpm, 5 min). 11S globulin fibril was prepared by synergistic enzymatic method mentioned above. The mixed solution was injected into glutaraldehyde solution (20 mL/L), stirred thoroughly, and allowed to react overnight at 4 °C in a refrigerator to prepare composite hydrogels [26]. Thereafter, the hydrogels prepared were all immersed in glutaraldehyde solution (20 mL/L) for 12 h to fix, and was washed with deionized water, and then frozen at $-80\,^{\circ}\text{C}$. Afterward, they were freeze-dried for 72 h to obtain the aerogels.

2.15. Microplastic removal by 11S globulin aerogels

The microplastic adsorption kinetics were tested at 25 $^{\circ}C$ and pH 7 according to the method of Zhuang et al. [27]. Aerogels of 6 mg were placed in a 5 mL polystyrene (PS) suspension (0.1 mg/mL). The fluorescence intensity of PS suspension with particle size of 1 μm was detected by fluorescence spectrophotometer (Hitachi Ltd., Tokyo, Japan) at 1, 3, 5, 10, 20, 30 min. The excitation and emission wavelengths were 528 nm and 588 nm, respectively. The amount of microplastics adsorbed by aerogel was calculated using the following equation:

$$q_t = \frac{(C_0 - C_t)V}{m} \tag{4}$$

 q_t is the adsorption capacity at time t. C_0 and C_t are the concentration of microplastics at 0 min and t min, respectively. m is the weight of the aerogel, and V is the volume of the microplastics solution.

To further investigate the distribution of microplastics within the aerogels, a laser confocal microscope was utilized. The composite aerogel was stained with FITC solution (10 mg/mL), and the stained aerogel was then placed on a glass slide for immediate observation using CLSM (ZESS 900, Zeiss, Göttingen, Germany) at an excitation/emission wavelength of 488/518 nm. This allowed for the visualization of PS microplastics adsorbed within the aerogel [28].

2.16. Adsorption of microplastics from beverages using aerogels

Plastic bottles containing coke, Sprite, and orange juice were placed in a 50 °C water bath for 2 h to facilitate microplastic migration. An aerogel sample (2 mg) was weighed and added to separate containers, each containing 5 mL of beverage. The containers were then placed in a 25 °C water bath for 2 h to facilitate microplastic adsorption by the aerogels, after which the aerogels were removed. The remaining solution was filtered using a glass fiber filter membrane with a pore size of 0.45 μm . The filter membrane was dried at 75 °C for 12 h prior to filtration, and its mass was documented as mo. The microplastics were collected using vacuum filtration. After the filter membrane was dried at

75 °C for 12 h, it was weighed again and recorded the mass as m_1 . In a control experiment, where no aerogel was used for adsorption in 5 mL of beverages, the weight of filter membrane before and after filtration was measured, recording the masses as m_A and m_B , respectively. The adsorption efficiency (AE) and adsorption capacity (AC) can be calculated according to the following formulas [3,29].

$$AE = \frac{(m_B - m_A) - (m_1 - m_0)}{(m_B - m_A)} \tag{5} \label{eq:5}$$

$$AC = \frac{m_1 - m_0}{W} \tag{6}$$

W (mg) represents the mass of the aerogel, $(m_1 - m_0)$ is the mass of microplastics adsorbed by the aerogel from the beverage, and $(m_B - m_A)$ is the total mass of microplastics in the beverage.

2.17. Statistical analyses

The experimental results were analyzed with IBM SPSS Statistics 26 and are expressed as mean \pm standard deviation of triplicate samples. Statistical significance was defined at p < 0.05.

3. Results and discussion

3.1. The effect of germination on the morphology of QPI aggregates and their fibrillation kinetics

We discovered that quinoa is easy to germinate under soaked conditions at room temperature (Fig. 2A) compared with mung bean and soy bean (Supplementary Fig. 1), and during the germination the endogenous enzymes are activated to hydrolyze storage proteins. It can be proposed that quinoa protein is hydrolyzed during germination that induces protein fibrillation at mild and sustainable conditions rather than the harsh conditions such as acidic hydrolysis and long-term heating. Therefore, the kinetics of QPI aggregation were monitored, and the cross-β-sheet of fibrillar protein was measured using thioflavin T (ThT) labeling [6]. An initial lag-free phase was observed in Fig. 2C, and all groups reached a plateau after heating for 30 min, indicating a fast fibrillation of QPI. Notably, the G0 (pH 2) sample showed comparable growth kinetics to the G8 (pH 7) sample, indicating that germination for 8 h (G8) is an appropriate condition to facilitate fibrillation of QPI. However, the extension of the germination time did not further enhance the fibrillation, and the ThT fluorescence intensity of G16 (pH 7) and G24 (pH 7) was significantly lower than that of the G8 (pH 7) sample. It was reported that quinoa protein is less prone to form fibrils compared with other plant proteins [12]. This could be due to that excessive

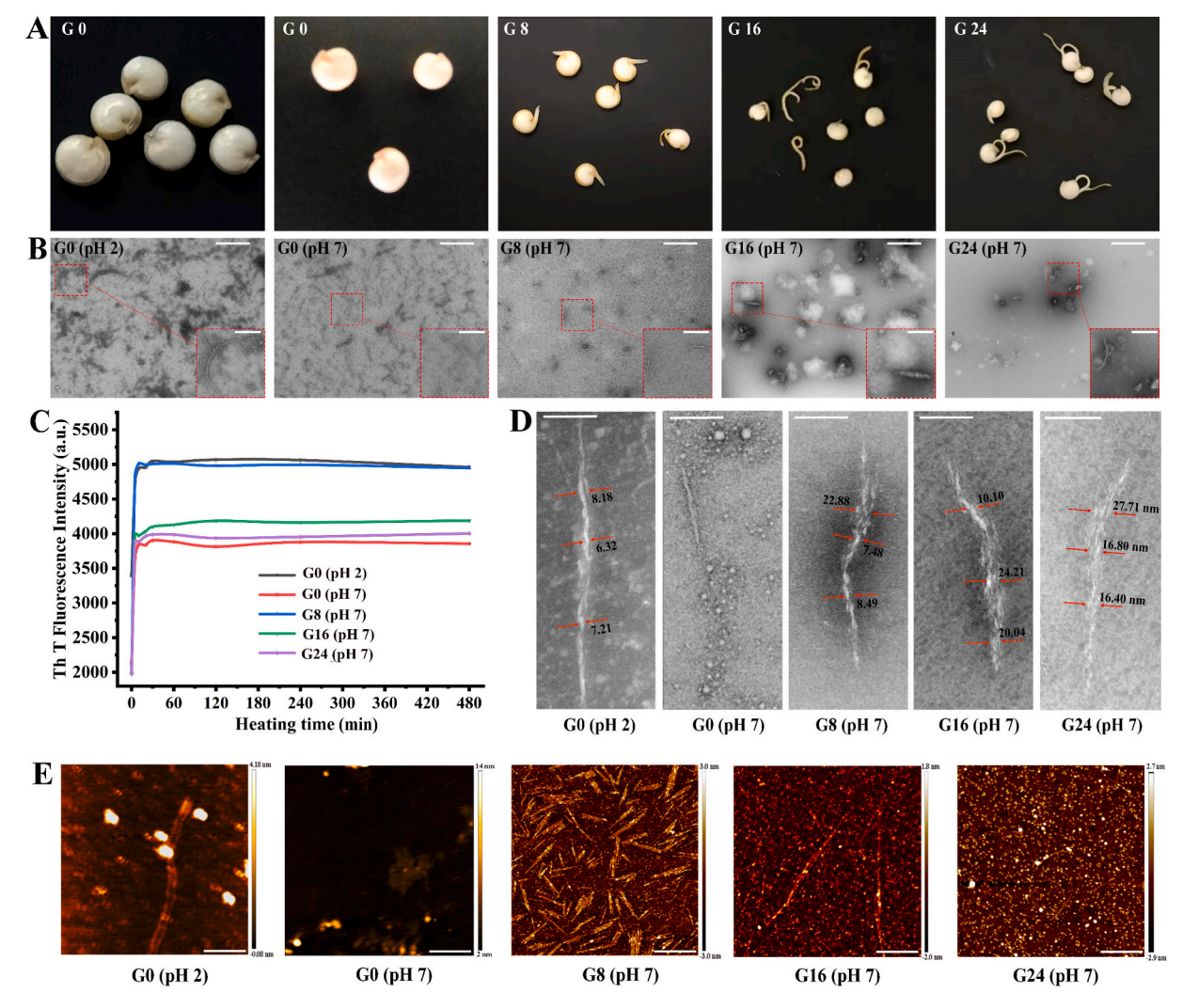


Fig. 2. The effect of germination on the morphology of QPI aggregates and their fibrillation kinetics. (A) Appearance of germinated quinoa. (B) TEM images of QPI aggregates, scale bars, 1 μm. Inset zoom image, scale bars, 500 nm. (C) Fibrillation kinetics of QPI. (D) The morphology of QPI fibrils, scale bars, 100 nm. (E) AFM images of QPI aggregates, scale bars, 400 nm. *G0, G8, G16, and G24 indicate QPIs extracted from quinoa germinated for 0, 8, 16, and 24 h, respectively.

heating (pH 2, 6–10 h) degraded the formed QPI fibrils [30].

We further examined the morphology of QPI aggregates and discovered that QPI extracted from quinoa germinated for 8 h formed 200–800 nm fibrils (Supplementary Fig. 2), while QPI aggregates were mainly globular particles at pH 7 when quinoa was ungerminated. Notably, short fibrils with a length of approximately 200 nm were formed after heating at pH 2 for 30 min (Supplementary Fig. 2). It is noteworthy that more amorphous aggregates were found in the G16 (pH 7) and G24 (pH 7) samples.

QPI fibrils in each sample were further enlarged to reveal their structure and are shown in Fig. 2D. The alteration of white and gray areas was observed, which indicates the relatively higher and lower regions and the helical structure of QPI fibrils. AFM images (Fig. 2E) provide 3D dimensions of QPI aggregates. G0 (pH 7) QPI aggregates showed particulate and amorphous morphology, and G0 (pH 2) QPI formed fibrillar aggregates with a height of approximately 2 nm (Supplementary Fig. 3). It is noticeable that germination facilitated QPI fibrillar aggregation, as abundant fibrils were observed in G8 (pH 7)

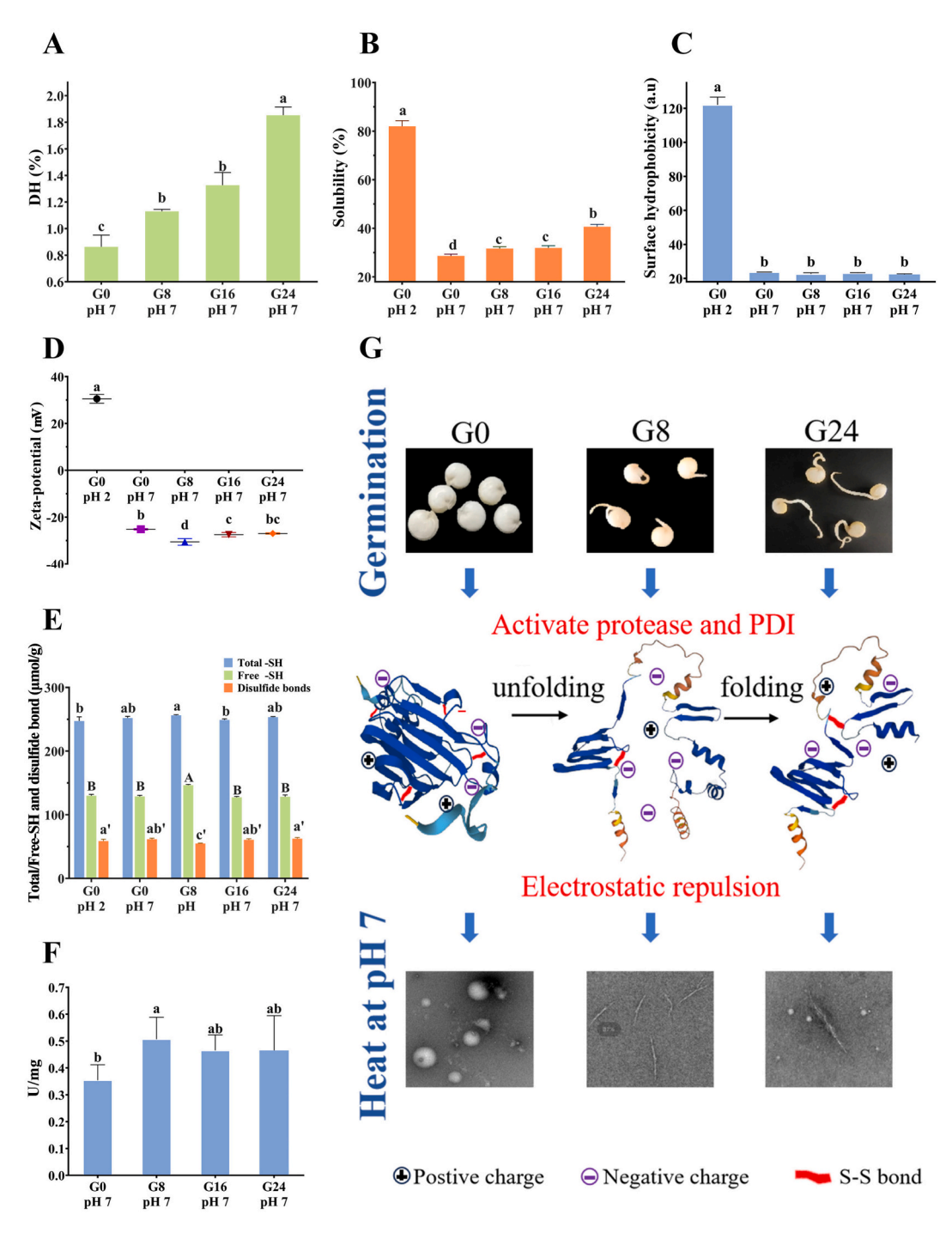


Fig. 3. Effects of germination on the physicochemical properties of QPIs. (A) Degree of hydrolysis. (B) Protein solubility. (C) Surface hydrophobicity. (D) Zeta potential. (E) Total/free sulfhydryl and disulfide bond content. (F) Disulfide bond reduction activity of protein disulfide isomerase extracted from quinoa germinated for 0, 8, 16, 24 h. (G) The mechanism of QPI fibrillation facilitated by germination. *Different lowercase and uppercase letters indicate significant differences (*P* < 0.05). In Fig. 3D, the significant difference of the absolute value of zeta-potential was evaluated. G0, G8, G16, and G24 indicate QPIs extracted from quinoa germinated for 0, 8, 16, and 24 h, respectively.

sample, which is consistent with TEM results.

3.2. The effects of germination on the physicochemical properties of QPIs

To reveal the reason why germination facilitated fibrillation, the study on the effects of germination on the physicochemical properties and composition of QPIs was carried out. As shown in Fig. 3A, the degree of hydrolysis (DH) of QPI gradually increased with the increasing germination time, as germination activated endogenous enzymes and hydrolyzed quinoa protein to peptides, which are the building blocks of aggregates [31,32]. The effects of germination on protein composition are presented in Supplementary Table 1, where the ungerminated (G0) sample exhibited significantly different compositions at pH 2 and 7. The reason is that the protein is susceptive to hydrolysis under acidic conditions. Under reducing conditions, the 11S acidic subunit remained basically unchanged with the increasing germination time, while the content of the alkaline subunit decreased from 25.51 % to 24.70 %.

At pH 7, the solubility of QPI increased with the increasing germination time (Fig. 3B). It could be favorable for protein fibrillation, as recruiting soluble protein molecules is crucial for templating similar structures to generate repetitive amyloid-like protein fibrils [33]. The surface hydrophobicity of proteins reflects the exposure of hydrophobic groups [15]. As the germination time extended, the surface hydrophobicity decreased gradually (Fig. 3C), which corresponded to the increase of solubility.

It was observed in Fig. 3D that germination generally increased the absolute value of the zetapotential of QPI, and G8 (pH 7) showed the highest absolute value at pH 7. The changes in zeta-potential can be attributed to surface modification of proteins [34]. During germination, quinoa protein was probably deamidated, which exposed carboxylic groups and increased the net negative charge of QPI [35]. With the extension of germination time, the hydrolysis of QPI cleaved the peptide bonds and altered the composition of QPI, leading to the variation in the electronegativity of QPI. Germination for 8 h improved the electronegativity of QPI, which enhanced the electrostatic repulsion between the proteins. With the increased repulsive force (electrostatic repulsion), the protein aggregation rate was slowed down, which was conducive to better orientation and arrangement of protein molecules, forming ordered fibrillar aggregates (Fig. 3G).

The sulfhydryl content reflects the protein conformation and its unfolding state. Fig. 3E indicates that G8 (pH 7) QPI exhibited the highest content of free sulfhydryl group and the lowest disulfide bond content. The increase in free sulfhydryl groups may result from the activated disulfide isomerase during germination, which can reduce disulfide bonds and unfold protein structure [36]. Cao et al. [37] reported that the reduction of disulfide bonds in globulin could promote fibrillar aggregation. Therefore, G8 (pH 7) showed a significant fibrillation in Fig. 2, as the unfolding of protein conformation provided sufficient conformational freedom for protein self-assembly. However, G16 (pH 7), G24 (pH 7) showed lower free sulfhydryl content and higher disulfide bond content, indicating the folding state of protein structure, which reduced the fibrillation of QPI. To verify this hypothesis, protein disulfide isomerase (PDI) was extracted from quinoa germinated for 0, 8, 16, 24 h, and the disulfide bond reduction activity was measured. G8 sample showed the highest disulfide bond reduction activity in Fig. 3F. Therefore, PDI played a vital role to unfold the protein conformation and facilitate the fibrillation.

However, the longer germination time (16, 24 h) reduced the electronegativity of QPI (Fig. 3D), which decreased the electrostatic repulsion thus enhanced the molecular interaction and aggregation rate. Moreover, the disulfide bond reduction is less significant in G16 (pH 7) and G24 (pH 7) QPI, leading to the folding of QPI structure and the weakening of the fibrillar assembly (Fig. 3G). In our study, electrostatic repulsion and disulfide bond reduction played an important role in determining aggregation behavior of QPI at pH 7.

3.3. Effects of gastrointestinal digestion on the morphology, ThT florescence intensity and cytotoxicity of QPI aggregates

To further reveal the effects of digestion on the structure of QPI aggregates, the changes of morphology and ThT fluorescence intensity of QPI aggregates after gastrointestinal digestion were studied. Fig. 4A shows that some fibrils of G0 (pH 2) and G8 (pH 7) can still be observed after gastric and intestinal digestion, respectively. However, amorphous aggregates were observed in G0 (pH 7) after gastric digestion, and disappeared after intestinal digestion, indicating amorphous aggregates are more prone to digestion compared with fibrillar aggregates. Fig. 4B indicates the changes of ThT fluorescence intensity of G0 (pH 7), G8 (pH 7) and G0 (pH 2) as a function of digestion time. After gastrointestinal digestion, the ThT fluorescence intensity finally decreased to 12.38 %, 16.27 % and 5.36 %, respectively, and the decrease occurred mainly in the gastric digestion phase. It indicated that most of the fibrils were digested at the simulated GI conditions.

As fibrillar structure was not fully disrupted after simulated digestion, the cytotoxicity of different QPI aggregates before and after gastrointestinal digestion to non-cancerous intestinal cell lines MODE-K cells was evaluated using the CCK-8 assay. As shown in Fig. 4C, the samples (G0 pH 2, G0 pH 7 and G8 pH 7) before digestion were essentially nontoxic. Meanwhile, G8 (pH 7) could promote cell proliferation to some extent, which might be attributed to protein fibrils mimicking the structural features of collagen fibrils (a main component of the extracellular matrix) and serving as a source of nutrients [38,39]. Moreover, the digestive juices of G0 (pH 2) and G8 (pH 7) were safe and biocompatible and even promoted cell growth to some extent. It is claimed by Raffaele Mezzenga that the digested lysozyme and β-lactoglobulin fibrils exhibit no observable cytotoxicity [40]. Furthermore, the digested food amyloids didn't cause physiological abnormalities nor inducing plaques in brain nor other organs. The in vitro and in vivo studies suggested that food amyloids are as safe as those digested native proteins.

3.4. Effects of germination on the gelling property of QPI

The effects of different aggregation behavior induced by germination on the appearance, gel microstructure and rheological properties of QPI gels were investigated. The homogeneous gels were formed for G0 (pH 2) and G8 (pH 7) with smooth and intact surface (Fig. 5A), while apparent pores were found in G0 (pH 7), G16 (pH 7) and G24 (pH 7) gels. Furthermore, the G0 (pH 2) and G8 (pH 7) gels possessed a homogeneous and dense gel network structure as visualized by CLSM (Fig. 5B), while apparent voids were observed in G0 (pH 7), G16 (pH 7) and G24 (pH 7) gels, decreasing the continuity of gel structure. Meanwhile, big aggregates were found in G0 (pH 7), G16 (pH 7) and G24 (pH 7) gels (Fig. 5B), which led to the heterogeneity of gel structure.

The rheological properties of QPI dispersions are shown in Fig. 5C, D. At pH 7, G' was lower than G" at the initial stage of heating, and rose sharply during the heating process. Among them, G8 sample had the highest G' at the end of heating, and it remained higher than the other samples during the subsequent holding and cooling process. Meanwhile, G8 QPI showed the lowest gelation temperature (T_{gel}) of 67.1 °C, while the T_{gel} of G0, G16 and G24 was 73.1, 69.1, 74.1 °C, respectively (Fig. 5E), indicating the enhanced gelling property of QPI via fibrillar aggregation. Furthermore, G8 (pH 7) QPI showed the lowest least gelation concentration (LGC) of 60 mg/mL among five groups (Fig. 5F), confirming the improved gelling property via fibrillation under pH 7. However, the LGC of G0 (pH 2) QPI was 100 mg/mL, which is probably due to the absence of disulfide bonds to form self-supporting gels.

3.5. Effects of enzyme synergy on the fibrillation of 11S globulin

Inspired by germination, two vital enzymes, protease and PDI were applied to modify the structure of quinoa 11S globulin, which accounts

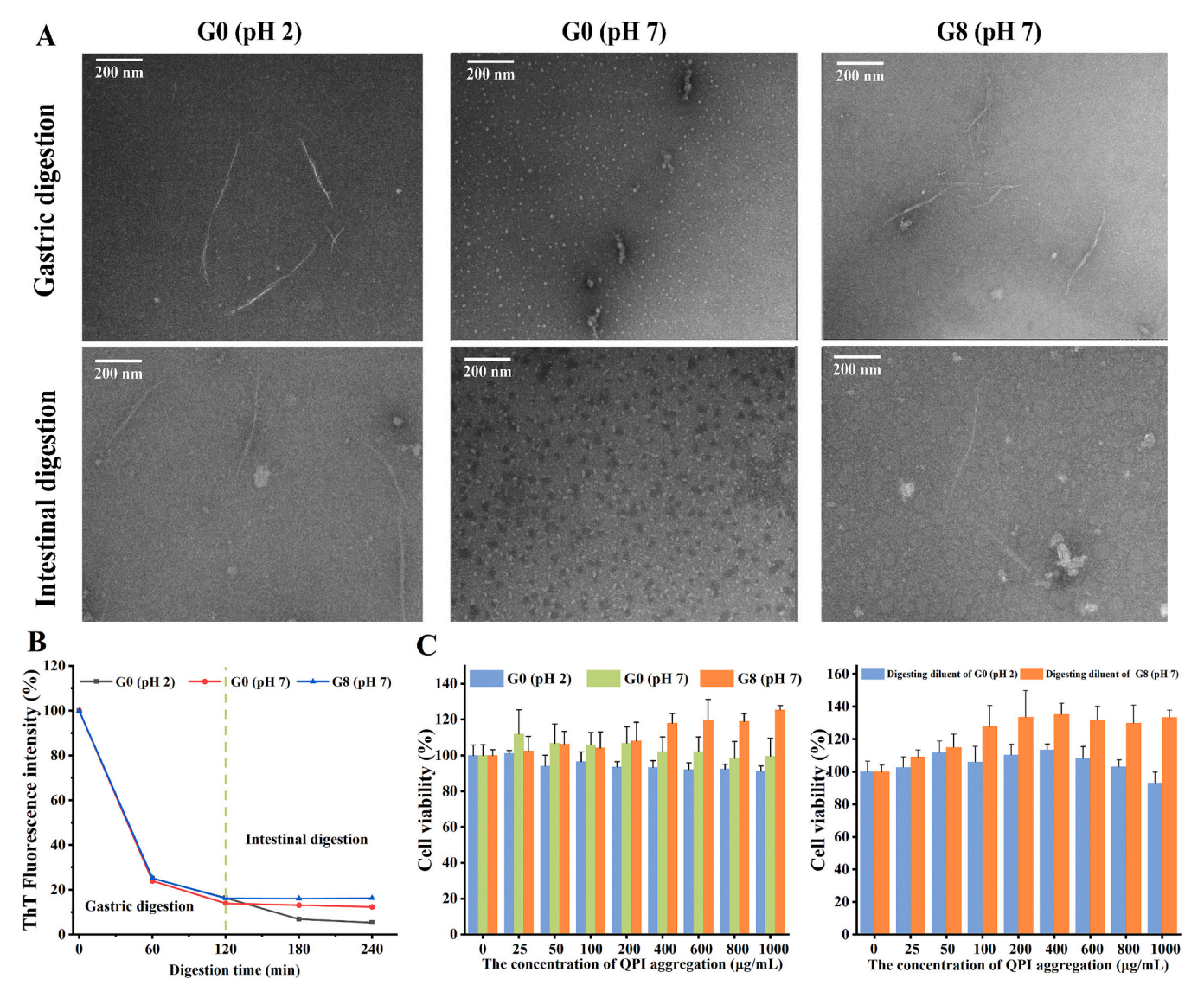


Fig. 4. Effects of gastrointestinal digestion on QPI aggregates. (A) The morphology of QPI aggregates after gastrointestinal (2 h) and intestinal digestion (2 h). (B) Normalized ThT fluorescence intensity of QPI aggregates as a function of digestion time. (C) Effects of gastrointestinal digestion on the cytotoxicity of QPI aggregates. *GO and G8 indicate aggregates generated from QPI extracted from quinoa germinated for 0 and 8 h, respectively.

for 37 % of quinoa protein. Although 2S albumin constitutes 35 % of quinoa protein, it was difficult to form fibrils as shown in Supplementary Fig. 4. It was also reported that globular proteins contained segments with high fibrillation tendency [41]. During germination, various proteases were activated, such as carboxypeptidase, cysteine protease, aspartic protease, serine protease and metalloproteases [42]. To simplify the proteolysis process, bromelain, a byproduct extracted from pineapple stems and peels, was chosen to hydrolyze quinoa 11S globulin in vitro. As we mentioned in Section 3.2, PDI played a vital role to unfold the protein conformation and facilitate the fibrillation. PDI extracted from quinoa seeds and bromelain were applied to simulate the effects of germination.

The effect of enzyme treatments on the 11S globulin fibrils' conversion rate was shown in Supplementary Fig. 5. The conversion rate increased after bromelain hydrolysis or PDI reduction compared with the group without enzyme treatment, indicating that bromelain hydrolysis and PDI reduction promoted the fibrillation of quinoa 11S globulin. Furthermore, we found that the conversion rate of the fibrils was 42.7 %, attributed to the synergistic effects of bromelain hydrolysis and PDI reduction. This was comparable to the 47 % conversion rate of fava bean protein isolate fibrils obtained through thermosonication at pH 2, and

was higher than that of whey protein fibrils formed at pH 2 (32 %) [43].

The morphology of quinoa 11S globulin amyloid-like fibrils was observed by TEM and AFM and shown in Fig. 6. Quinoa 11S globulin formed worm-like fibrillar aggregates after heating at pH 2. Meanwhile, mainly particulate and amorphous aggregates were formed in the absence of enzyme treatment (Supplementary Fig. 6). Notably, bromelain hydrolysis of 11S globulin significantly increased the formation of fibrillar aggregates after thermal treatment, which showed typical rigid or semiflexible fibrils' morphology. The average contour length was 546.2 nm, which was significantly longer than the 11S globulin fibrils formed at pH 2 (114.9 nm).

The formation of rigid and semiflexible fibrils was also stimulated by PDI treatment alone, and the average length was 507.8 nm. It is noteworthy that bromelain hydrolysis cooperated with PDI reduction leading to the formation of the longest and most abundant fibrils, with an average length of 2907.6 nm. The morphology was also rigid or semiflexible fibrils. It is worthy to mention that some spherical particles with a diameter of about 8–13 nm were presented in all TEM images. Martinez et al. [44] reported that the diameter of quinoa 11S globulin was approximately $11\,\pm\,2$ nm. Therefore, these spherical particles were quinoa 11S globulin which were not aggregated. There was less 11S

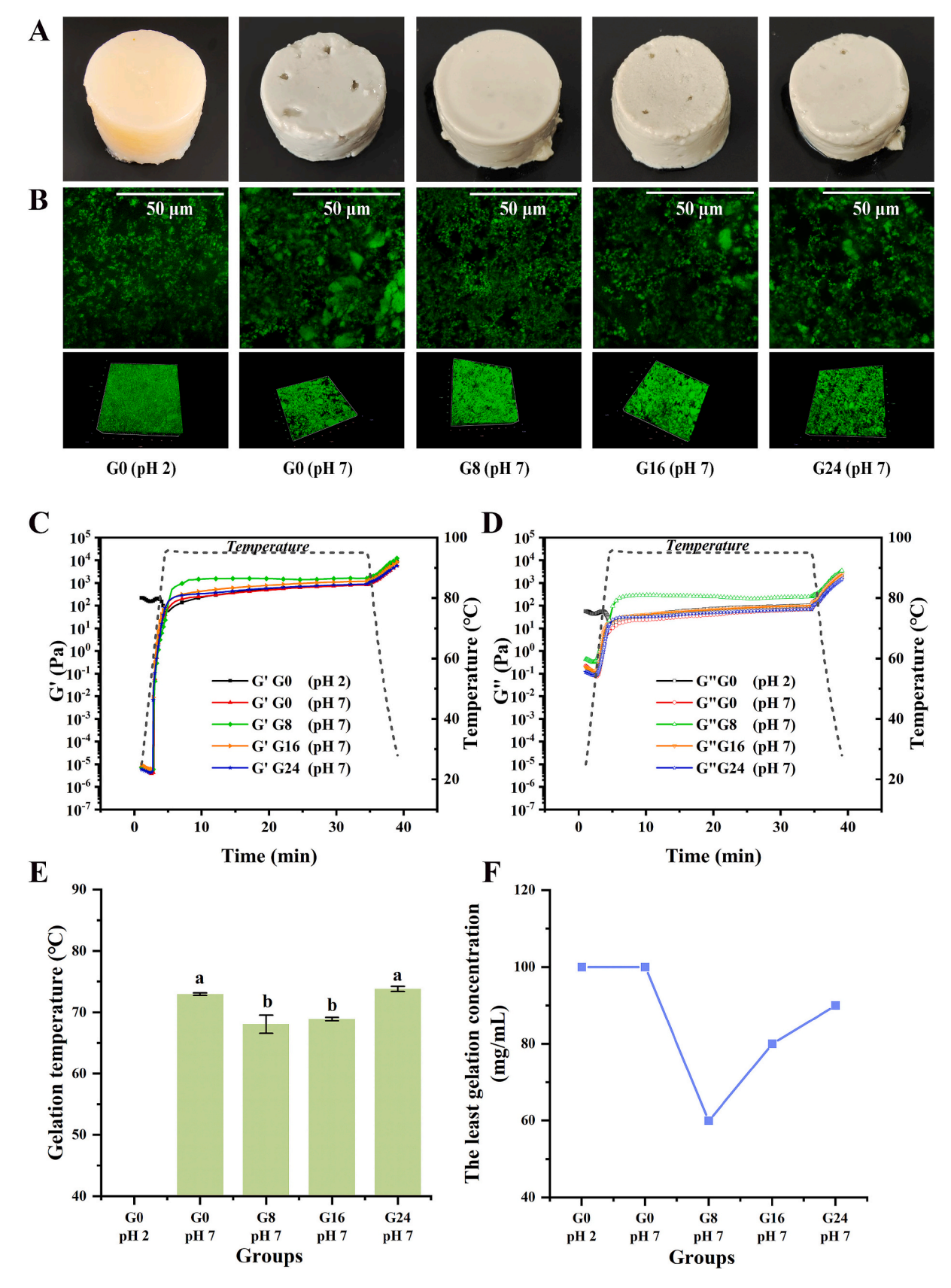


Fig. 5. The effects of germination on the gelling properties of QPIs. (A) Appearance and microstructure (B) of QPI gels. The rheological properties (C, D), the gelation temperature (E), and the lowest gelation concentration (F) of QPI dispersions.

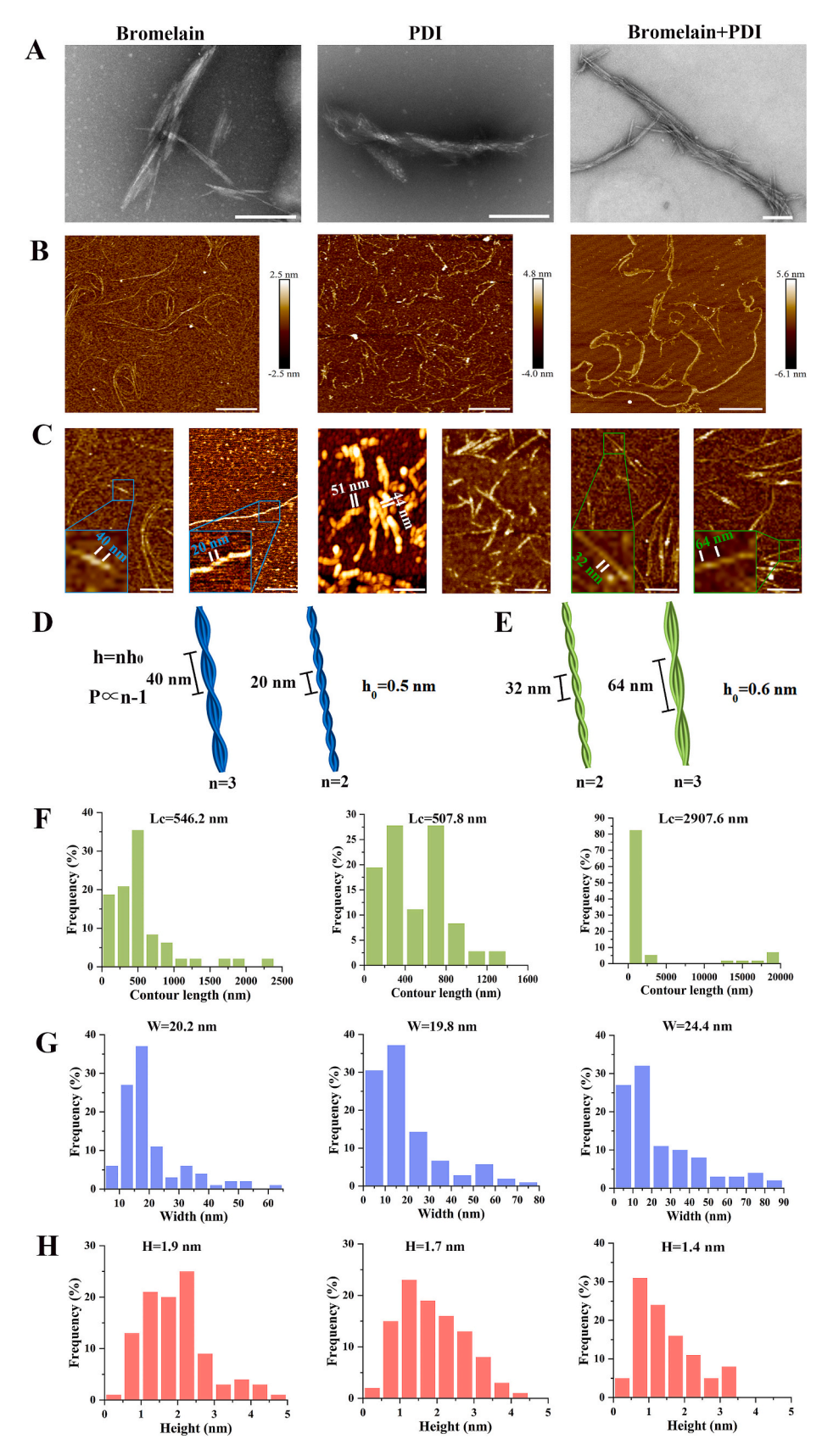


Fig. 6. TEM, AFM and statistical analysis of quinoa 11S globulin fibrillar aggregates with various enzyme treatments. (A) TEM images, scale bars, 200 nm. (B) AFM images, scale bars, 1 μ m. (C) Magnified AFM images, scale bars, 300 nm. Schematic illustration of the helical fibrils induced by bromelain (D) and bromelain + PDI (E) treatment. (F) Contour length distribution. (G) Width distribution. (H) Height distribution. *h represents the maximum height of the fibril, and h_0 represents the height of the protofibril. n represents the number of protofibrils, and P represents the periodic pitch of fibril.

globulin under the synergistic treatment of bromelain and PDI, as more 11S globulin monomers were involved in the formation of protein fibrils, resulting in higher numbers and longer fibrils, as well as higher conversion rate.

FTIR is widely employed for determining the secondary structure of proteins. As shown in Table 1, when bromelain hydrolysis was cooperated with PDI reduction, the highest β -sheet content (a characteristic of amyloid fibril formation) was observed in the aggregates, reaching 54.2 %, followed by the sample treated with bromelain hydrolysis (47.25 %) and PDI reduction (44.09 %) individually. Meanwhile, the content of random coils in aggregates diminished after enzymatic treatment. The transformation from random coils to β -sheets indicated that more fibrillar aggregates were formed in the bromelain + PDI group. Notably, the stretching vibration peak of O—H in the aggregates underwent red shift after enzymatic treatment, with the peak in the bromelain + PDI group reaching 3292.71 cm $^{-1}$ (Supplementary Fig. 7). This indicated that hydrogen bonds were pivotal in the formation of fibrils.

Moreover, the periodic pitch of most fibrils increased with the increasing height, which is consistent with previous reports [45,46]. However, some fibrils have a larger periodic pitch but shorter height, which can be attributed to the influence of chirality, electrostatic interactions, and mechanical stress on the twisting of protein fibrils [4]. Intriguingly, under the synergistic action of bromelain and PDI, it was found that when the periodic pitch of the protein fibrils was 32 nm and 64 nm, the corresponding maximum heights were 1.2 nm and 1.8 nm, respectively. This suggests that fibrils with heights of 1.2 nm and 1.8 nm were formed by the twisting and coiling of 2 and 3 protofibrils, and the height of protofibril was 0.6 nm. This is because the maximum height (h) of the fibril is proportional to the number of protofibrils (n) that constitute it, which means $h \approx n h_0. \; h_0$ represents the height of a single protofibril. Additionally, the periodic pitch of the protein fibrils is proportional to n-1 [45]. Linear relation between the periodic pitch of 11S globulin fibrils and n-1 was also observed in bromelain induced fibrils. The fibril with a periodic pitch of 40 nm was composed of three protofibrils, each with an ho of 0.5 nm, whereas the fibril with a periodic pitch of 20 nm consisted of two protofibrils.

Intriguingly, both left-handed and right-handed fibrils were observed in bromelain, PDI, and bromelain + PDI treated groups. This is due to the diversity of amino acids sequences in 11S globulin, as a pair of acidic and basic subunit in 11S globulin is comprised of 479 amino acids. Different building blocks may contribute to the left-handed and right-handed fibrils as observed by AFM. It was reported by Usov and Mezzenga et al. [47] that both left-handed and right-handed bovine serum albumin fibrils were observed.

The cysteine content in quinoa 11S globulin is relatively low, which is only 1.00 g/100 g as shown in Supplementary Table 2. Even though the sulfhydryl groups are not pronated under pH 7, there is less formation of disulfide bonds during heating due to the limited cysteine content in 11S globulin, which can facilitate the formation of ordered protein fibrils [37]. The content of aromatic amino acids in 11S globulin is 7.62 g/100 g, which is comparable to that of lentil protein at 7.50 g/100 g and chickpea protein at 7.90 g/100 g, both of which are known to

Table 1 Secondary structure of quinoa 11S globulin aggregates.

Groups	Secondary structure (%)			
	α-Helix	β-Sheet	Random coils	β-Turn
Without enzyme	12.75 ± 0.43^{a}	35.14 ± 5.04^{c}	24.57 ± 0.75^{a}	30.87 ± 1.02^{a}
Bromelain	$11.33 \; \pm \\ 0.84^a$	$47.25 \pm \\ 1.55^{\rm b}$	$\begin{array}{c} 12.03 \; \pm \\ 0.42^c \end{array}$	28.7 ± 0.16^{a}
PDI	$11.97 \pm \\ 0.82^a$	$44.09 \pm \\ 2.62^{b}$	$14.77 \pm 0.93^{\mathrm{b}}$	29.16 ± 3.51^{a}
Bromelain + PDI	$\begin{array}{c} 11.54 \pm \\ 0.18^{ab} \end{array}$	54.20 ± 1.66^{a}	11.50 ± 0.83^{c}	$\begin{array}{l} 29.16 \pm \\ 3.51^{a} \end{array}$

readily form protein fibrils [13]. Tyrosine, 3.11 g/ 100 g in quinoa 11S globulin, its carboxy-terminal peptide bond is one of the cleavage sites that bromelain prefers to hydrolyze. The presence of tyrosine at the C-terminus can facilitate protein fibrillation through π - π stacking and the formation of aromatic ladder [48].

3.6. The microplastic removal by aerogels

Microplastics are widely present in foods packaged by plastics, and microplastics can be accumulated in human bodies to increase the risk of inflammation and various diseases. Therefore, microplastics removal by food grade materials is desired to decrease their intake. The optimization of quinoa 11S globulin fibrillation laid solid foundation to structure aerogels with promising porosity and surface area (Fig. 7A, B).

However, aerogels composed solely of 11S globulin fibrils were prone to disintegration upon exposure to water. To address this issue, chitosan was incorporated to produce composite aerogels. Fig. 7F shows the microplastic adsorption capacity of aerogels as a function of time with different mass ratios between 11S globulin fibrils and chitosan. Within the first 10 min, the adsorption of microplastic particles by the aerogels was rapid due to the abundant adsorption sites within the aerogel and the capillary action. As the adsorption time increased, the microplastic adsorption by aerogels gradually increased and reached an equilibrium at approximately 20 min. In Fig. 7F, the maximum adsorption capacity was 33.2 mg/g for chitosan aerogels, which was significantly higher than 26.7 mg/g for aerogels generated from quinoa 11S globulin fibrils. According to existing research, the isoelectric point of polystyrene is pH 3.96. When the pH of the dispersion system was above pH 3.96, polystyrene microspheres possessed a negative charge [49]. At pH 7.0, chitosan has positive charge, while 11S globulin fibrils have a negative charge. Therefore, the chitosan aerogels exhibited a stronger electrostatic adsorption effect on microplastics.

As the mass ratio of 11S globulin fibrils to chitosan increased, the positive charges on the chitosan surface were progressively neutralized by the negative charges on the protein fibrils, leading to a slight decrease in the electrostatic adsorption of microplastics by the composite aerogels. The maximum adsorption capacities of the 11SF + CS (1:1) and 11SF + CS (2:1) aerogels were 27.3 mg/g and 31.2 mg/g, respectively. Although the adsorption capacity decreased, the addition of 11SF increased the formation of network structures in the aerogels as shown in Fig. 7B &C, providing more binding sites for microplastics [50]. When the mass ratio of 11SF to CS was 3:1, the microplastic adsorption reached a maximum value of 54.4 mg/g, which was significantly higher than that of other aerogels. Notably, the 11SF + CS (3:1) aerogels exhibited the highest surface area, as shown in Supplementary Fig. 8 A, which contributed to a more pronounced network structure in the aerogel and provided additional binding sites for microplastics, as evidenced in Fig. 7D. Although Wang et al. (2021) reported that their oat protein sponge (OPS) could rapidly adsorb 38 % of microplastics from a solution within 10 s, its maximum adsorption capacity was only 6.579 mg/g, which is considerably lower than the adsorption capacity of quinoa 11S globulin aerogels and 11SF/CS aerogels [49].

Fig. 7H illustrates the effect of aerogels on the adsorption capacity of microplastics in coke, Sprite and orange juice. CS, 11SF, and 11SF + CS (3:1) aerogels were all capable of adsorbing microplastics from both coke, Sprite and orange juice. Compared to the individual CS and 11SF aerogels, 11SF + CS (3:1) aerogel exhibited the best adsorption performance. Specifically, its adsorption efficiency and capacity for microplastics reached 44.8 % and 286.7 mg/g in coke, 53.3 % and 457.5 mg/g in Sprite, and 50.0 % and 370.9 mg/g in orange juice, respectively (Fig. 7I). This improvement can be attributed to the larger specific surface area (Supplementary Fig. 8) and more pronounced network structure of the aerogel, which provides more available sites for microplastic adsorption [49]. The conclusion and underlying mechanism of this study are summarized in Fig. 8.

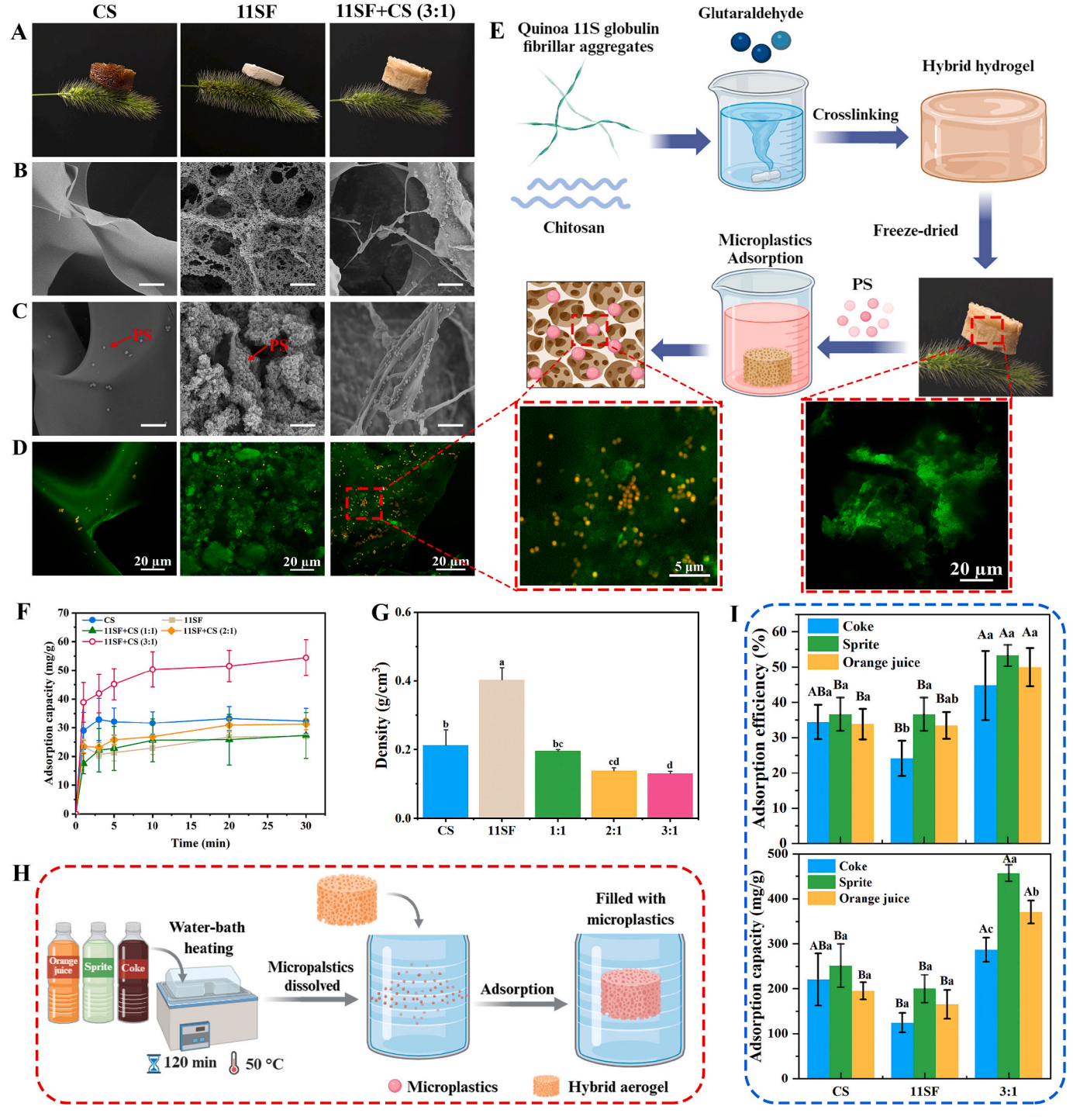


Fig. 7. Characterization and microplastics adsorption of aerogels. (A) Photographs of light aerogels on top of setaria viridis. (B, C) SEM images of aerogels before and after adsorption of microplastics. Scale bar, 20 μm. (D) CLSM images of aerogels after adsorption of microplastics. Scale bar, 20 μm. (E) Schematic illustration of the synthesis process and microplastics adsorption of hybrid aerogel. (F) Microplastics adsorption capacity versus time at an initial concentration of 100 ppm. (G) Density of aerogels. (H) Schematic illustration of the microplastics adsorption of hybrid aerogel in three beverages. (I) The effect of aerogels on the adsorption efficiency and adsorption capacity of microplastics in different beverages. *Letters a-c and A-C in Fig. 7I denote statistically significant differences in microplastic adsorption among different beverages by the same type of aerogel, and within the same beverage by different types of aerogels, respectively.

4. Conclusion

This research firstly reported an innovative method for quinoa protein fibrillation under neutral condition. We found that quinoa germination hydrolyzed protein and unfolded its structure via disulfide bond reduction, which facilitated QPI fibrillation. The increased electronegativity of QPI after 8 h germination could enhance the repulsive force

and ordered orientation of protein, leading to fibrillation of QPI. Meanwhile, quinoa protein fibrillation at pH 7 enhanced its gelling property, and QPI fibrils showed biosafety before and after gastrointestinal digestion. However, the extended germination induced particulate aggregation, which decreased the hardness and G' of QPI gels. Inspired by germination, two vital enzymes were applied to modify the structure of quinoa 11S globulin and facilitate fibrillation, with the

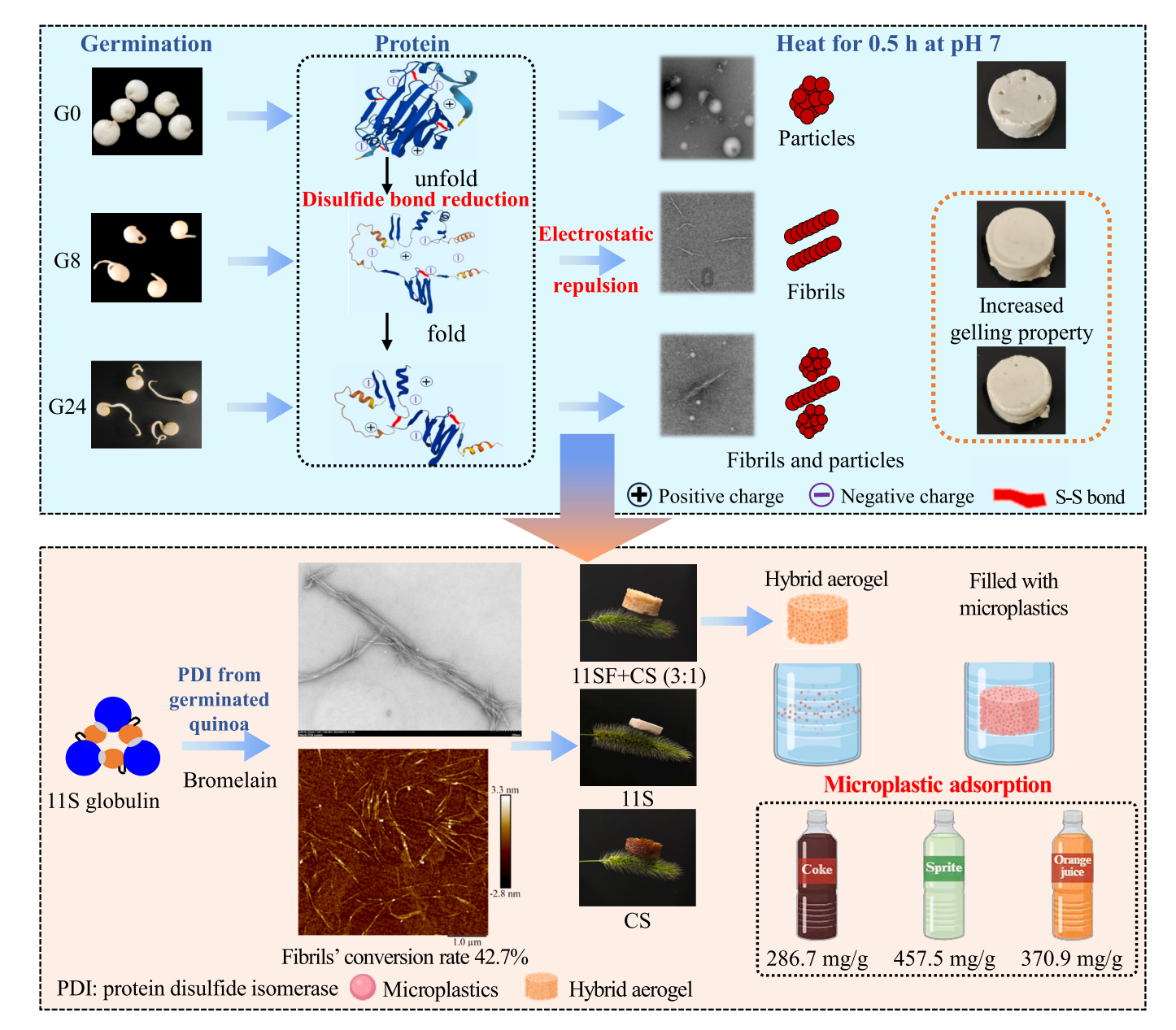


Fig. 8. Mechanistic illustration of germination-induced fibril nanoarchitectonics of quinoa protein at neutral pH and its aerogel application for microplastic removal.

fibrils' conversion rate reaching 42.7 %. It's worth mentioning that aerogels formed by 11S globulin fibrils were effective to remove microplastics in water and beverages, indicating its practical application. This finding contributes to the green processing of quinoa protein, which is of great significance for plant-based protein industry and microplastic removal.

CRediT authorship contribution statement

Xiao Feng: Writing – review & editing, Supervision, Funding acquisition, Conceptualization. Lixiao Fu: Writing – original draft, Visualization, Methodology, Investigation. Jianfeng Wei: Methodology, Investigation. Chaosheng Wu: Writing – original draft, Visualization, Methodology, Investigation. Hui Zhang: Methodology, Investigation. Lin Chen: Visualization. Xi Yu: Writing – review & editing, Methodology. Yuan Li: Writing – review & editing, Supervision, Conceptualization. Xiaozhi Tang: Writing – review & editing, Supervision, Conceptualization.

Declaration of competing interest

The authors declare that they have no known competing financial interests or personal relationships that could have appeared to influence the work reported in this paper.

Acknowledgments

This research was funded by the National Natural Science Foundation of China (NSFC32372380), and the Outstanding Youth Foundation of Jiangsu Province (BK20240143), and the Priority Academic Program Development of Jiangsu Higher Education Institutions (PAPD).

Appendix A. Supplementary data

Supplementary data to this article can be found online at https://doi. org/10.1016/j.jcis.2025.139058.

Data availability

No data was used for the research described in the article.

References

- L.F. Amato-Lourenço, R. Carvalho-Oliveira, G.R. Júnior, L. dos Santos Galvão, R. A. Ando, T. Mauad, Presence of airborne microplastics in human lung tissue, J. Hazard. Mater. 416 (2021) 126124, https://doi.org/10.1016/j. ihazmat.2021.126124.
- [2] Z. Yan, Y. Liu, T. Zhang, F. Zhang, H. Ren, Y. Zhang, Analysis of microplastics in human feces reveals a correlation between fecal microplastics and inflammatory bowel disease status, Environ. Sci. Technol. 56 (2021) 414–421, https://doi.org/ 10.1021/acs.est.1c03024.
- [3] B.Y. Zheng, B. Li, H. Wan, X.F. Lin, Y.P. Cai, Coral-inspired environmental durability aerogels for micron-size plastic particles removal in the aquatic environment, J. Hazard. Mater. 431 (2022) 128611, https://doi.org/10.1016/j. ibazmat 2022 128611
- [4] J. Zhou, T. Li, M. Peydayesh, M. Usuelli, V. Lutz-Bueno, J. Teng, L. Wang, R. Mezzenga, Oat plant amyloids for sustainable functional materials, Adv. Sci. 9 (4) (2021) 2104445, https://doi.org/10.1002/advs.202104445.
- [5] M. Pieper, A. Michalke, T. Gaugler, Calculation of external climate costs for food highlights inadequate pricing of animal products, Nat. Commun. 11 (2020) 6117, https://doi.org/10.1038/s41467-020-19474-6.
- [6] J. Ge, C. Sun, S. Li, N. Deng, Y. Zhang, Y. Fang, Fibrillization kinetics and rheological properties of panda bean (*Vigna umbellata (Thunb.) Ohwi et Ohashi*) protein isolate at pH 2.0, Int. J. Biol. Macromol. 228 (2022) 816–825, https://doi. org/10.1016/j.foodchem.2022.133016.
- [7] D. Zhang, X. Wei, Z. Liu, X. Wu, C. Bao, Y. Sun, N. Su, J. Cui, Transcriptome analysis reveals the molecular mechanism of GABA accumulation during quinoa (*Chenopodium quinoa* Willd.) germination, J. Agric. Food Chem. 69 (41) (2021) 12171–12186. https://pubs.acs.org/doi/10.1021/acs.jafc.1c02933.
- [8] R. Parsons, Incidence and ecology of very fast germination, Seed Sci. Res. 22 (2012) 161–167, https://doi.org/10.1017/s0960258512000037.
 [9] S. Liu, W. Wang, H. Lu, Q. Shu, Y. Zhang, Q. Chen, New perspectives on
- [9] S. Liu, W. Wang, H. Lu, Q. Shu, Y. Zhang, Q. Chen, New perspectives on physiological, biochemical and bioactive components during germination of edible seeds: a review, Trends Food Sci. Technol. 123 (2022) 187–197, https://doi.org/ 10.1016/i.tifs.2022.02.029.
- [10] M. Liu, M. Childs, M. Loos, A. Taylor, L.B. Smart, A. Abbaspourrad, The effects of germination on the composition and functional properties of hemp seed protein isolate, Food Hydrocoll. 134 (2023) 108085, https://doi.org/10.1016/j. foodbyd 2022 108085
- [11] Z. Yang, L. de Campo, E.P. Gilbert, R. Knott, L. Cheng, B. Storer, X. Lin, L. Luo, S. Patole, Y. Hemar, Effect of NaCl and CaCl₂ concentration on the rheological and structural characteristics of thermally-induced quinoa protein gels, Food Hydrocoll. 124 (2022) 107350, https://doi.org/10.1016/j.foodhyd.2021.107350.
- [12] M.R. Nilsson, Techniques to study amyloid fibril formation in vitro, Methods 34 (2004) 151–160. https://doi.org/10.1016/j.ymeth.2004.03.012.
- (2004) 151–160, https://doi.org/10.1016/j.ymeth.2004.03.012.
 [13] T. Li, J.T. Zhou, M. Peydayesh, Y. Yao, M. Bagnani, I. Kutzli, Z.X. Chen, L. Wang, R. Mezzenga, Plant protein amyloid fibrils for multifunctional sustainable materials, Adv. Sustain. Syst. 7 (4) (2023) 2200414, https://doi.org/10.1002/adsu.202200414.
- [14] P.M. Nielsen, D. Petersen, C. Dambmann, Improved method for determining food protein degree of hydrolysis, J. Food Sci. 66 (5) (2001) 642–646, https://doi.org/ 10.1111/j.1365-2621.2001.tb04614.x.
- [15] Y. Di, X. Li, X. Chang, R. Gu, X. Duan, F. Liu, X. Liu, Y. Wang, Impact of germination on structural, functional properties and in vitro protein digestibility of sesame (*Sesamum indicum* L.) protein, LWT-Food Sci. Technol. 154 (2022) 112651, https://doi.org/10.1016/j.lwt.2021.112651.
- [16] A.K. Anderson, P.K.W. Ng, Changes in disulfide and sulfhydryl contents and electrophoretic patterns of extruded wheat flour proteins, Cereal Chem. 77 (3) (2000) 354–359, https://doi.org/10.1094/cchem.2000.77.3.354.
- [17] M. Lassé, D. Ulluwishewa, J. Healy, D. Thompson, A. Miller, N. Roy, K. Chitcholtan, J.A. Gerrard, Evaluation of protease resistance and toxicity of amyloid-like food fibrils from whey, soy, kidney bean, and egg white, Food Chem. 192 (2016) 491–498, https://doi.org/10.1016/j.foodchem.2015.07.044.
- [18] W. Bao, C.L. Lyu, B. Li, L.Y. Zhang, X.W. Liu, F. Li, D. Li, X. Gao, X. Shi, Y. Li, Experimental and theoretical explorations of nanocarriers' multistep delivery performance for rational design and anticancer prediction, Sci. Adv. 7 (2021) eaba2458, https://doi.org/10.1126/sciadv.aba2458.
- [19] A. Koh, K. Nishimura, R. Urade, Relationship between endogenous protein disulfide isomerase family proteins and glutenin macropolymer, J. Agric. Food Chem. 58 (24) (2010) 12970–12975, https://doi.org/10.1021/jf103347p.
- [20] D. Chen, O.H. Campanella, Limited enzymatic hydrolysis induced pea protein gelation at low protein concentration with less heat requirement, Food Hydrocoll. 128 (2022) 10754, https://doi.org/10.1016/j.foodhyd.2022.107547.
- [21] K. Kainuma, T. Ookura, Y. Kawamura, Purification and characterization of protein disulfide isomerase from soybean, J. Biochem. 117 (1) (1995) 208–215, https://doi.org/10.1093/oxfordjournals.jbchem.a124712.
- [22] A.M.R. Huyst, L.J. Deleu, T. Luyckx, L. Van der Meeren, J.A.J. Housmans, C. Grootaert, M. Monge-Morera, J.A. Delcour, A.G. Skirtach, F. Rousseau, J. Schymkowitz, K. Dewettinck, P. Van der Meeren, Impact of heat and enzymatic treatment on ovalbumin amyloid-like fibril formation and enzyme-induced

- gelation, Food Hydrocoll. 131 (2022) 107784, https://doi.org/10.1016/j.
- [23] X. Qi, Y. Li, W. Zhang, M. Shen, Y. Chen, Q. Yu, J. Xie, Proteolysis improves the foaming properties of rice protein fibrils: structure, physicochemical properties changes, and application in angel food cake, Food Chem. 437 (2024) 137765, https://doi.org/10.1016/j.foodchem.2023.137765.
- [24] C. Wu, W. Ma, Y. Chen, W.B. Navicha, D. Wu, M. Du, The water holding capacity and storage modulus of chemical cross-linked soy protein gels directly related to aggregates size, LWT–Food Sci. Technol. 103 (2019) 125–130, https://doi.org/ 10.1016/j.lwt.2018.12.064.
- [25] S. Nagireddi, V. Katiyar, R. Uppaluri, Pd(II) adsorption characteristics of glutaraldehyde cross-linked chitosan copolymer resin, Int. J. Biol.Macromol. 94 (2017) 72–84, https://doi.org/10.1016/j.ijbiomac.2016.09.088.
- [26] M.E.I. Badawy, N.E.M. Taktak, O.M. Awad, S.A. Elfiki, N.E.A. El-Ela, Preparation and characterization of biopolymers chitosan/alginate/gelatin gel spheres crosslinked by glutaraldehyde, J. Macromol. Sci B. 56 (2017) 359–372, https://doi. org/10.1080/00222348.2017.1316640.
- [27] J. Zhuang, M. Pan, Y. Zhang, F. Liu, Z. Xu, Rapid adsorption of directional cellulose nanofibers/3-glycidoxypropyltrimethoxysilane/polyethyleneimine aerogels on microplastics in water, Int. J. Biol. Macromol. 235 (2023) 123884, https://doi.org/ 10.1016/j.ijbiomac.2023.123884.
- [28] C. Zhang, N. Yue, X. Li, H. Shao, J. Wang, L. An, F. Jin, Potential translocation process and effects of polystyrene microplastics on strawberry seedlings, J. Hazard. Mater. 449 (2023) 131019, https://doi.org/10.1016/j.jhazmat.2023.131019.
- [29] Y.H.B. Yang, Z.X. Liu, C.H. Yin, Z.M. Han, Q.F. Guan, Y.X. Zhao, Z.C. Ling, H.C. Liu, K.P. Yang, W.B. Sun, S.H. Yu, Edible, ultrastrong, and microplastic-free bacterial cellulose-based straws by biosynthesis, Adv. Funct. Mater. 32 (15) (2021) 211713, https://doi.org/10.1002/adfm.202111713.
- [30] Z. Wei, Q. Huang, In vitro digestion and stability under environmental stresses of ovotransferrin nanofibrils, Food Hydrocoll. 99 (2020) 105343, https://doi.org/ 10.1016/j.foodhyd.2019.105343.
- [31] Y. Lan, W. Zhang, F. Liu, L. Wang, X. Yang, S. Ma, Y. Wang, X. Liu, Recent advances in physiochemical changes, nutritional value, bioactivities, and food applications of germinated quinoa: a comprehensive review, Food Chem. 426 (2023) 136390, https://doi.org/10.1016/j.foodchem.2023.136390.
- [32] K. Ariga, Nanoarchitectonics: the method for everything in materials science, B Chem Soc Jpn. 97 (1) (2024) uoad001, https://doi.org/10.1093/bulcsj/ uoad001.
- [33] R. Riek, D.S. Eisenberg, The activities of amyloids from a structural perspective, Nature 539 (2016) 227–235, https://doi.org/10.1038/nature20416.
- [34] K. Müntz, M. Belozersky, Y. Dunaevsky, A. Schlereth, J. Tiedemann, Stored proteinases and the initiation of storage protein mobilization in seeds during germination and seedling growth, J. Exp. Bot. 52 (2001) 1741–1752, https://doi. org/10.1093/jexbot/52.362.1741.
- [35] M.I. Mahmoud, W.T. Malone, C.T. Cordle, Enzymatic hydrolysis of casein: effect of degree of hydrolysis on antigenicity and physical properties, J. Food Sci. 57 (5) (1992) 1223–1229, https://doi.org/10.1111/j.1365-2621.1992.tb11304.x.
- [36] D.B. Medinas, P. Rozas, C. Hetz, Critical roles of protein disulfide isomerases in balancing proteostasis in the nervous system, J. Biol. Chem. 298 (7) (2022) 102087, https://doi.org/10.1016/j.jbc.2022.102087.
- [37] Y. Cao, J. Adamcik, M. Diener, J.R. Kumita, R. Mezzenga, Different folding states from the same protein sequence determine reversible vs irreversible amyloid fate, J. Am. Chem. Soc. 143 (30) (2021) 11473–11481, https://doi.org/10.1021/ iacs.1c03392.
- [38] X. Jia, J. Song, W. Lv, J.P. Hill, J. Nakanishi, K. Ariga, Adaptive liquid interfaces induce neuronal differentiation of mesenchymal stem cells through lipid raft assembly, Nat. Commun. 13 (1) (2022) 3110, https://doi.org/10.1038/s41467-022-30622-v.
- [39] X. Liu, X. Jin, P. Ma, Nanofibrous hollow microspheres self-assembled from starshaped polymers as injectable cell carriers for knee repair, Nat. Mater. 10 (2011) 398–406, https://doi.org/10.1038/nmat2999.
- [40] D. Xu, J. Zhou, W.L. Soon, I. Kutzli, A. Molière, S. Diedrich, M. Radiom, S. Handschin, B. Li, L. Li, S.J. Sturla, C.Y. Ewald, R. Mezzenga, Food amyloid fibrils are safe nutrition ingredients based on in-vitro and in-vivo assessment, Nat. Commun. 14 (1) (2023) 6806, https://doi.org/10.1038/s41467-023-42486-x.
- [41] J. Song, K. Kawakami, K. Ariga, Localized assembly in biological activity: origin of life and future of nanoarchitectonics, Adv. Colloid Interface Sci. 339 (2025) 103420, https://doi.org/10.1016/j.cis.2025.103420.
- [42] F.A. Guzmán-Ortiz, J. Castro-Rosas, C.A. Gómez-Aldapa, R. Mora-Escobedo, A. Rojas-León, M.L. Rodríguez-Marín, R.N. Falfán-Cortés, A.D. Román-Gutiérrez, Enzyme activity during germination of different cereals: a review, Food Rev. Int. 35 (3) (2018) 177–200, https://doi.org/10.1080/87559129.2018.1514623.
- [43] C. Sun, C. Wang, Z. Xiong, Y. Fang, Properties of binary complexes of whey protein fibril and gum arabic and their functions of stabilizing emulsions and simulating mayonnaise, Innovative Food Sci. Emerg. Technol. 68 (2021) 102609, https://doi. org/10.1016/j.ifset.2021.102609.
- [44] J.H. Martínez, F. Velázquez, H.P. Burrieza, K.D. Martínez, A. Paula Domínguez Rubio, C. Dos Santos Ferreira, M. Del Pilar Buera, O.E. Pérez, Betanin loaded nanocarriers based on quinoa seed 11S globulin. Impact on the protein structure and antioxidant activity, Food Hydrocoll. 87 (2019) 880–890, https:// doi.org/10.1016/j.foodhyd.2018.09.016.
- [45] J. Adamcik, J.M. Jung, J. Flakowski, P. De Los Rios, G. Dietler, R. Mezzenga, Understanding amyloid aggregation by statistical analysis of atomic force microscopy images, Nat. Nanotechnol. 5 (6) (2010) 423–428, https://doi.org/ 10.1038/nnano.2010.59.

- [46] M. Wang, P. Zhou, J. Wang, Y. Zhao, H. Ma, J.R. Lu, H. Xu, Left or right: how does amino acid chirality affect the handedness of nanostructures self-assembled from short amphiphilic peptides? J. Am. Chem. Soc. 139 (11) (2017) 4185-4194, https://doi.org/10.1021/jacs.7b00847
- [47] I. Usov, R. Mezzenga, FiberApp: An open-source software for tracking and analyzing polymers, filaments, biomacromolecules, and fibrous objects, Macromolecules 48 (5) (2015) 1269–1280, https://doi.org/10.1021/ma502264c. [48] Q. Xu, Y. Ma, Y. Sun, D. Li, X. Zhang, C. Liu, Protein amyloid aggregate: structure
- and function, Aggregate 4 (4) (2023) e333, https://doi.org/10.1002/agt2.333.
- [49] Z. Wang, C. Sun, F. Li, L. Chen, Fatigue resistance, re-usable and biodegradable sponge materials from plant protein with rapid water adsorption capacity for microplastics removal, Chem. Eng. J. 415 (2021) 129006, https://doi.org/ 10.1016/j.cej.2021.129006.
- [50] N. Nematidil, M. Sadeghi, S. Nezami, H. Sadeghi, Synthesis and characterization of Schiff-base based chitosan-g-glutaraldehyde/NaMMTNPs-APTES for removal Pb $^{2+}$ and Hg $^{2+}$ ions, Carbohydr. Polym. 222 (2019) 114971, https://doi.org/10.1016/j.carbpol.2019.114971.